High Activity and Efficient Turnover by a Simple, Self-Assembled "Artificial Diels–Alderase"

High Activity and Efficient Turnover by a Simple, Self-Assembled "Artificial Diels–Alderase"

Vicente Martí-Centelles, Andrew L. Lawrence and Paul J. Lusby*

EaStCHEM School of Chemistry, University of Edinburgh, Joseph Black Building, David Brewster Road, Edinburgh, Scotland, UK. EH9 3FJ. E-mail: Paul.Lusby@ed.ac.uk.

ABSTRACT: The Diels–Alder (DA) reaction is a cornerstone of synthesis, yet Nature does not use catalysts for intermolecular [4+2] cycloadditions. Attempts to create artificial "Diels–Alderases" have also met with limited success, plagued by product inhibition. Using a simple Pd_2L_4 capsule we now show DA catalysis that combines efficient turnover alongside enzyme-like hall-marks. This includes excellent activity ($k_{cat}/k_{uncat} > 10^3$), selective transition-state (TS) stabilization comparable to the most proficient DA catalytic antibodies, and control over regio- and chemo-selectivity that would otherwise be difficult to achieve using small-molecule catalysts. Unlike other catalytic approaches that use synthetic capsules, this method is not defined by entropic effects; instead multiple H-bonding interactions modulate reactivity, reminiscent of enzymatic action.

Introduction

Creating artificial catalysts that rival the levels of activity and selectivity exhibited by enzymes remains challenging. A biomimetic approach defined by using a microenvironment superficially reminiscent of an enzyme active site is one-way researchers have chosen to tackle this challenge.[1] In this regard, self-assembled systems are appealing because the construction of chemical microenvironments requires a macromolecular design, most easily realized using reversible, weak interactions to bring together smaller components in a three-dimensional array.[2]

A common theme to emerge from investigations with various "supramolecular" catalyst systems is the use of entropic mechanisms to underpin reactivity. Using multi-substrate encapsulation to achieve high effective concentration of species is an established concept, first exemplified by Breslow using cyclodextrins.[3] Later, Kelly,[4] Rebek[5] and Sanders[6] all showed that bimolecular reactions could be similarly accelerated using synthetic covalent receptors capable of binding multiple reactants. However, these and more recent studies with the self-assembled systems of Rebek[7], Fujita[8] and others[9] have revealed that catalysis is frequently halted before even one turnover is complete due to tight product binding. This has been particularly common with cycloaddition reactions (Figure 1a), where the 100% atom efficiency reinforces product inhibition, although rare exceptions are known.[10] As a result, the recent trend in capsule catalysis has been to select reactions, such as hydrolysis,[11] ring openings[12] and sigma-tropic rearrangements,[13] on the basis that the products show the same or preferably weaker affinity than the substrates. The avoidance of using capsules to catalyze annulation reactions exposes a weakness in current methods.

In addition to entropic effects, including constrictive binding[13] and increased effective concentration through ion-pairing,[12b] coulombic stabilization of charged intermediates by cationic, anionic and even neutral capsules has also been invoked to explain rate enhancement.[1e,14] Nonetheless, the cavities of most synthetic capsules lack polar functional groups that could provide direct interactions with either reactant(s) or transition state (TS), in the same way an enzyme would use a collection of polar amino acid residues. In contrast, we envisaged a new approach in which multiple non-covalent interactions would modulate reactivity (Figure 1b). This exploits a novel guest-binding approach recently described with the simple Pd_2L_4 capsule, **C-1**,[15a] wherein pockets of electron deficient H-atoms (Figure 1c, shown in blue) form interactions with complementary guests such as quinones.[15b] The increased reactivity of the dienophile would therefore arise due to a lowering of the guest LUMO energy—akin to H-bond organocatalysis.[16,17] An internalized and activated enone would eliminate the need to co-bind the diene, thereby decreasing product inhibition effects, whilst still giving the capsule microenvironment opportunity to influence both reactivity and selectivity.

Results and Discussion

Initial tests of this catalytic strategy focused on the DA reaction of benzoquinone, **1**, with a few small dienes (isoprene, **2**; cyclopentadiene **3**; cyclohexadiene, **4**). However, the results using 20 mol% **C-1** were not encouraging, showing no discernible acceleration compared to the control reactions (Figures 2a and S1; black squares uncatalyzed, red triangles with **C-1**). Considering possible capsule modifications, we envisaged that the *endo*-pyridyl variant,[15c] **C-2** (Figure 1c), should retain similar LUMO-lowering properties. However, it was also reasoned that the lone pair could destabilize substrate binding by replacing ArH···π with less favorable n···π interactions. As thermodynamic stabilization of reactants has a detrimental effect on the catalytic activation barrier ($\Delta G^{\ddagger}_{cat}$), we were hopeful that **C-2** could show increased reactivity. We were thus pleased to observe that 20 mol% **C-2** gave a pronounced increase in the rate of production of the cycloadducts **5**–**7** (Figures 2a and S1; green triangles), and that each catalyzed reaction proceeded smoothly to completion. While the stark difference in reactivity from almost identical capsules highlights the subtleties of developing enzyme-like catalysts, the lack of activity from **C-1** is also a useful control. Firstly, it likely eliminates catalysis from residual Lewis acidic Pd^{2+} ions. It also hints that there is no contribution from the interaction of **1** with the outer *ortho*-pyridyl H-

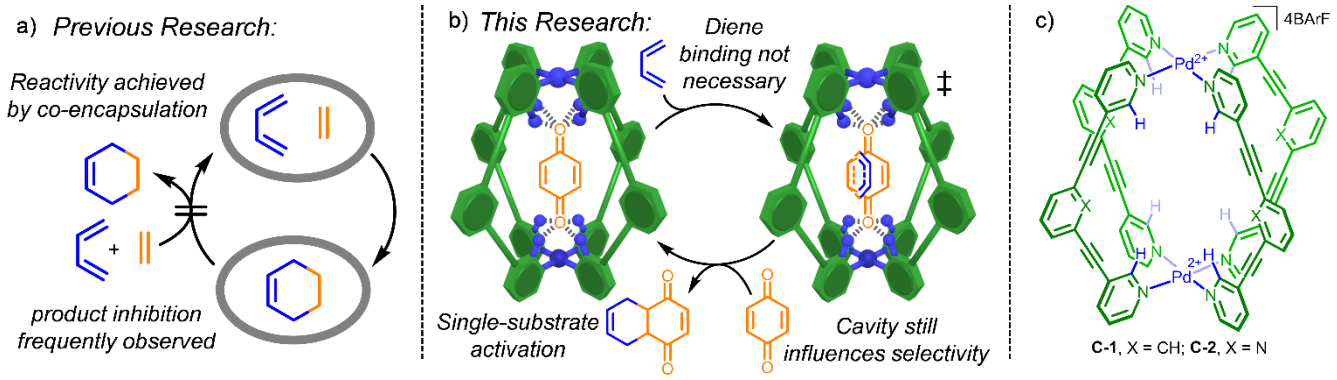

Figure 1. (a) Previous intermolecular DA capsule catalysis has utilized co-encapsulation. (b) Our approach utilizes internal dienophile polarization. (c) Pd_2L_4 capsules, **C-1** and **C-2**, used in this study.

bond donor sites. The confirmation that DA activity is dependent on quinone-encapsulation was obtained by adding excess competitive inhibitor, anthraquinone, which almost completely stops any acceleration (Figures 2a and S1, yellow circles).

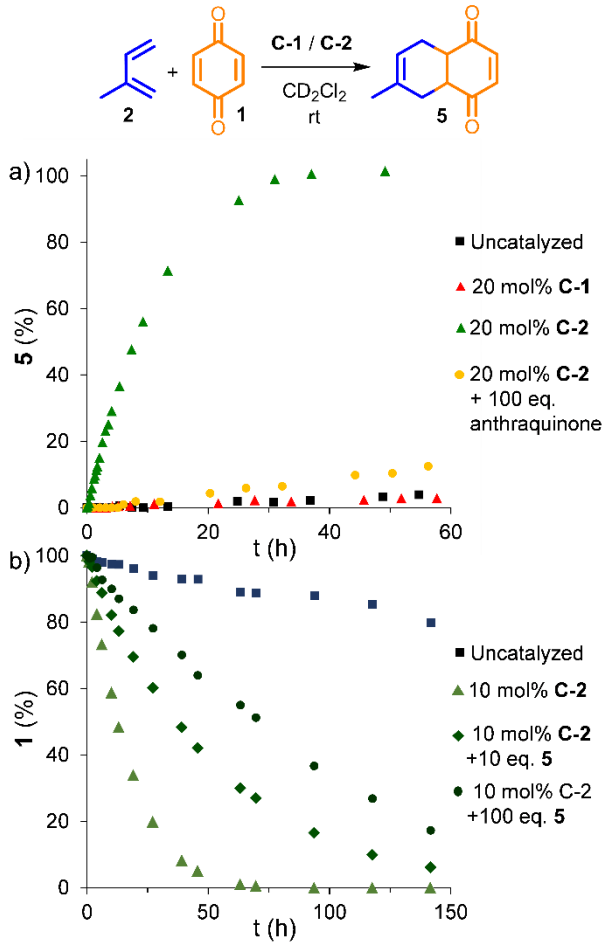

Figure 2. (a) Representative DA kinetic data. While **C-2** gives a marked acceleration (green triangles), structurally similar **C-1** (red triangles) gives no enhancement over the uncatalyzed reaction (black squares). **C-2** catalysis is retarded with anthraquinone (yellow circles) showing dienophile encapsulation necessary. (b) **C-2** (10 mol%) still accelerates DA of **1** and **2** with up to 100 eq. of product **5** added, showing 10^3 turnovers are feasible.

As expected, **C-2** binds substrate **1** less well (K_A = 1100 M^{-1}) in comparison to **C-1** (K_A = 8000 M^{-1}). However, substrate stabilization effects—wherein **C-1** "deactivates" **1** by 1.2 kcal mol^{-1} in comparison to **C-2** (Figure 3a)—only partly explain the difference in DA activity. Specifically, **C-2** appears much better suited to TS recognition,[18] as evidenced by the significantly tighter binding of conformationally locked adduct **6** (K_A = 11000 M^{-1}), which is a close structural mimic of the TS, and only binds weakly to **C-1** (K_A = 550 M^{-1}). Combining more effective TS stabilization—1.8 kcal mol^{-1} based on TS mimic **6**—with less favorable substrate binding (1.2 kcal mol^{-1}) would give an estimate of 3 kcal mol^{-1} difference in catalytic activation barriers ($\Delta G^{\ddagger}_{cat}$) for **C-1** and **C-2** based on measured thermodynamic parameters alone. The ^{1}H NMR titration data for **6** and **C-2** (Figure S36) also showed that several of the more H-bond acidic atoms of **6** exhibit large downfield shifts ($\Delta\delta$ > 1 ppm). This is consistent with the formation of favorable n···CH capsule-product, and by extension, capsule-TS interactions, thus providing a plausible structural rationale for the difference in reactivity between such similar capsules (Figure 3a).

To calculate the **C-2** rate enhancements (k_{cat}/k_{uncat}), we have used a non-linear analysis that involves fitting total dienophile consumption and/or product formation to a simulation based on a simple kinetic model (see SI). This considers the contribution from the uncatalyzed reaction (k_{uncat}), the rate of ingress and egress of substrate and product, as well as the 2nd order reaction of [**1**⊂**C-2**] with dienes **2**–**4** (k_{cat}). Utilizing the substrate and product K_A values as ratios of in-out rates, and assuming these are significantly quicker than cycloaddition (based on the time-averaged NMR spectra), yielded k_{cat} values that are listed in Table S1. Additionally, k_{cat}/k_{uncat} for the reaction of quinone **1** with dienes **2-4** are graphically represented in Figure 4a. The k_{cat}, k_{uncat} and $K_{A\ (quinone)}$ values have also been used to calculate the TS stabilization energies (ΔG_{TS}; Figure 3a, Table S2), which relates to the TS association constant ($K_{A\ TS}$; Figure 4), sometimes referred to as catalytic proficiency ($K_{A(quinone)} \cdot k_{cat}/k_{uncat}$). This analysis reveals that the binding strength of the TS mimic **6** significantly underestimates the acceleration afforded to the reaction of **1** and **3** by **C-2** (see above), as the energy barrier is lowered by more than 2 kcal mol^{-1} compared to $\Delta G_{product}$ (Figure 3a). It is even more apparent that **C-2** selectively stabilizes an early TS with the DA reaction of acyclic diene **2** (Figure 3b). Here, the significant TS stabilization is maintained even though the flexibility of product **5** allow conformational re-organization resulting in weak adduct binding (K_A = 500 M^{-1}).[19] With this reaction also fulfilling an ideal catalytic scenario, we have probed how many cycles are feasible.

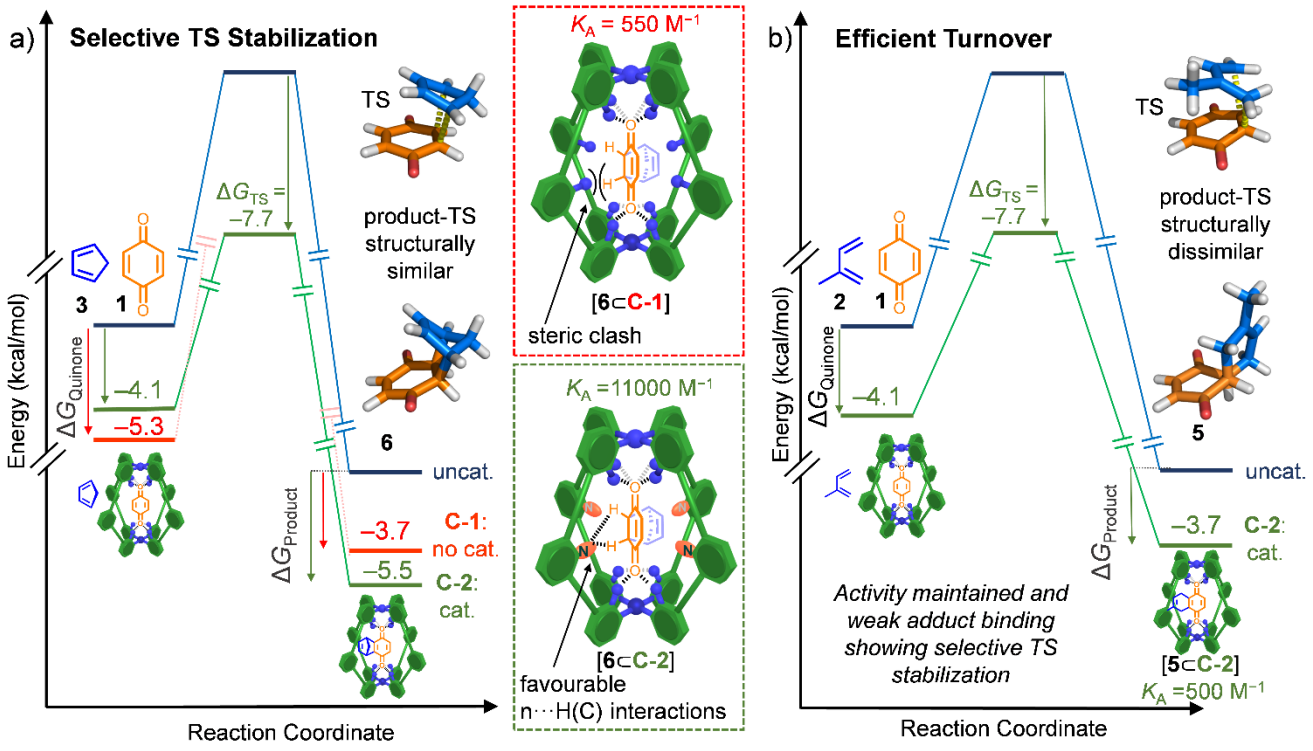

Figure 3. "Diels–Alderase" activity rationalized using substrate and TS stabilization effects. (a) DA activity correlates with TS mimic **6** binding affinities; stabilizing interactions with the *endo*-pyridyl groups of **C-2** are key. These lone pairs also destabilize substrate binding (n···π). (b) Similar acceleration with acyclic diene **2** to give weak binding adduct **5** shows that **C-2** stabilizes an "early" TS. Substrate / product / TS stabilization energies calculated from experimentally determined K_A, k_{cat} and k_{uncat} values.

This was done using conditions that give negligible background reaction (Figure 2b; 3 mM **1**, 30 mM **2**; blue squares) so that the substrate consumption: **C-2** loading ratio approximates to turnover number (TON). Under these conditions, 10 mol% **C-2** (0.3 mM) still gave full conversion in 48 hours (Figure 2b, green triangles: TON ≈ 10). However, reducing capsule concentration further gave an impracticably slow reaction. To avoid increasing the rate of the bulk-phase DA reaction, we therefore charged pre-prepared **5** to the start of each DA reaction to simulate low **C-2** loading. Significantly, when 10 eq. and even 100 eq. of **5** were added, consumption rates of **1** still proved superior relative to the uncatalyzed process (Figure 2b, dark green diamonds / circles). This latter experiment replicates the last 1% of a 0.1 mol% capsule-mediated reaction, demonstrating that TONs of 1000 are feasible. It is also worth noting that **6** is likely the worse-case scenario for this catalytic model in terms of product inhibition (similar but less pronounced effects are also seen with the other constrained adduct **7**) because of the structural similarity with the TS. Even in this case, the 20 mol% catalyzed **1** + **3** → **6** still goes smoothly to completion (Figure S1). It is likely that the sudden drop in activity that has characterized many other capsule-promoted cycloadditions is avoided because of the combination of good activity[20] and rapid substrate-product exchange. Indeed, simulation of this catalytic model at 20 mol% loading shows clearly that higher activity promotes more tolerance towards higher binding products (Figure 5).

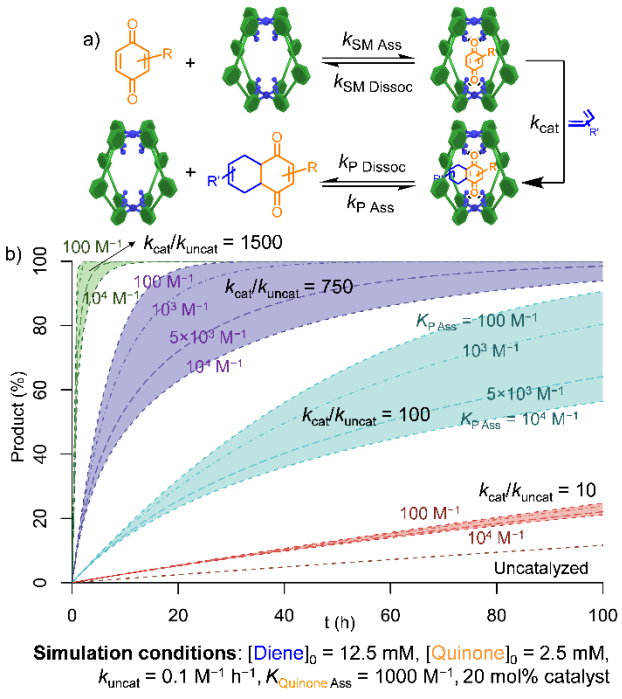

Figure 5. (a) The catalytic model under study. (b) Simulation of the cage catalyzed Diels–Alder reaction as a function activity (k_{cat}/k_{uncat} = 10 (red); 100 (turquoise); 750 (purple); 1500 (green)) and product binding strength ($K_{P\,Ass}$=100, 10^3, 5×10^3 and 10^4 M^{-1}.

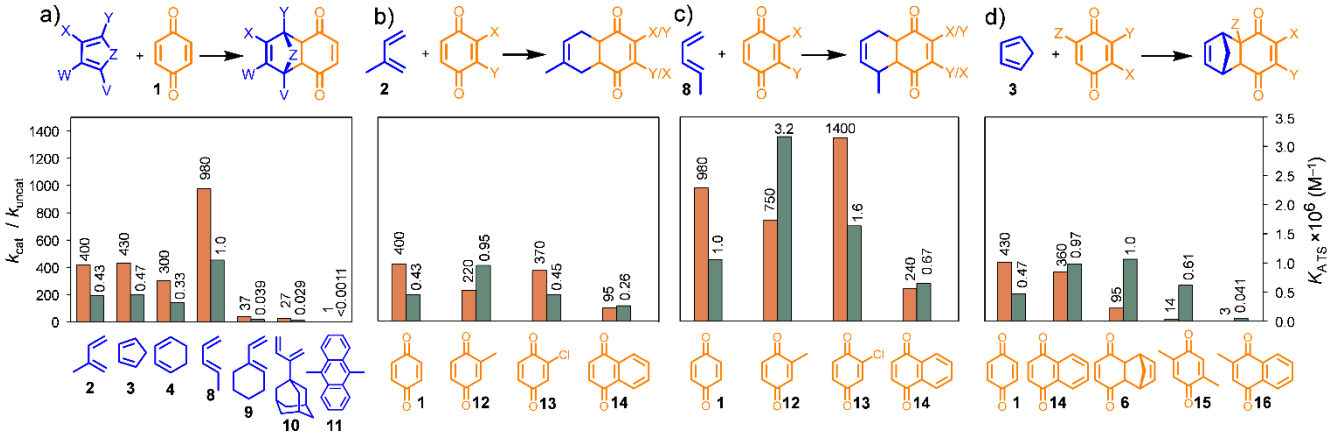

Figure 4. k_{cat}/k_{uncat} and $K_{A\ TS}$ values for a series of DA reactions where either the diene or dienophile is systematically varied. (a) The reduction in activity for bulky dienes **9**-**11** provides clear evidence for the necessary ingress of this component. (b-c) With small, acyclic dienes good-excellent activity is observed for a range of quinone dienophiles. (d) With increasing quinone size, reduced activity (k_{cat}/k_{uncat}) does not correlate with poor TS stabilization, rather stronger substrate binding. $K_{A\ TS}$ calculated from experimental K_A, k_{cat} and k_{uncat} values.

The influence the microenvironment has upon reactivity became apparent when the substrate scope was expanded (Figure 4). Initially focusing on diene variation (Figure 4a), comparing **2** to isomeric 1,3-pentadiene, **8**, a more-than doubling in k_{cat}/k_{uncat} to almost 10^3 was observed, a significant difference for such a subtle substrate change. To demonstrate the necessity of diene ingress, larger substrates were also screened. We were initially surprised to see that some activity is retained with dienes **9** and **10**, however, the complete lack of acceleration with reactive **11** provides strong evidence that catalytic action involves cycloaddition of the cavity-bound quinone. Turning to dienophile variation, isomeric dienes **2** and **8** were selected for further exploration (Figures 4b–c). These experiments revealed that catalysis is tolerant to modest increases in quinone size, wherein a single small substituent (e.g. **12** and **13**) makes little difference and even with naphthoquinone, **14**, reasonable activity is retained. These experiments also showed that **8** is a universally better diene with several dienophiles, the reactions with **1**, **12** and **13** all giving excellent k_{cat}/k_{uncat}, with values ranging from 750-1400. It is worth noting that the smallest acceleration of these three reactions (**8** + **12**) counterintuitively possess the highest TS stabilization, with a $K_{A\ TS}$ of 3.2×10^6 M^{-1}. Rather, lower acceleration is due to the greater affinity of substrate **12** (K_A = 4300 M^{-1}), which offsets the better TS stabilization. Similar effects are observed when the size of quinone is increased further (Figure 4d). For instance, 2,5-dimethyl-benzoquinone, **15**, exhibits a much more modest k_{cat}/k_{uncat} of 14. While it could have been assumed that this poorer catalytic effect was due to the restricted environment disfavoring tertiary bond formation, this is in fact not the case. Rather, the TS stabilization is greater than that afforded to the reaction of unsubstituted **1** with the same diene (i.e., **1** + **3** → **6**). Instead, the relatively poor k_{cat}/k_{uncat} is a consequence of the unusually high quinone K_A value of **15** (43000 M^{-1}), further exemplifying the subtle interplay between reactant and TS stabilization effects.

It has been revealing to compare the efficiency of **C-2** to other non-covalent DA catalysts. While our k_{cat}/k_{uncat} values are not directly comparable to many other "artificial Diels–Alderases" because of the discrepancy in units, a more universal analysis has been described by Houk that uses the difference between TS and reactant stabilization energies ($\Delta\Delta G$).[21] By this measure, the catalytic antibody 1E9 that catalyzes the reaction of maleimide and thiophene dioxide substrates is considered one of the most efficient non-covalent DA catalysts, with $\Delta\Delta G = -4.0$ kcal mol^{-1}. Significantly, the $\Delta\Delta G$ for the reaction of **8** and **13** catalyzed by **C-2** is −4.3 kcal mol^{-1}, with several other examples possessing values of –3.5 kcal mol^{-1} or better. Careful consideration should be applied when comparing such different systems, from solvent effects through to the disparity between catalysts that pre-bind one or both DA reactions partners. For example, the greater reduction in $\Delta G^{\ddagger}_{cat}$ in the case of **C-2** can be partly explained by a catalytic model that only involves dienophile stabilization, unlike 1E9 that binds and therefore lowers the energy of both reactants. Conversely, the entropic contribution to $\Delta G^{\ddagger}_{cat}$ for **C-2** will be greater than with systems that bind both diene and dienophile. Nonetheless, it is clear that **C-2** is very proficient at catalyzing the DA reactions of quinones with small dienes. We have also measured the thermodynamic and kinetic parameters associated with DA catalysis by a prototypical H-bond catalyst, the trifluoromethylaryl substituted thiourea first reported by Schreiner (see SI).[16] This is a useful comparison because of the similarity in the bimolecular catalytic step (k_{cat}). The data we have collected for the thiourea-catalyzed DA reaction of methyl vinyl ketone (K_A = 12 M^{-1}) with **3** shows a relatively modest k_{cat}/k_{uncat} of 41. As could be expected from the significantly fewer non-covalent interactions involved, the stabilization afforded both the reactant and the TS state (−1.5 and −3.6 kcal mol^{-1}, respectively) are much weaker in the case of the small molecule H-bond donor system. Consequently, such catalysts often only function at relatively high substrate concentrations (typically 100 mM dienophile, with excess diene). In contrast, **C-2** accelerates DA reactions under much more dilute conditions (2.5 mM dienophile), also minimizing contributions from any background process.

While Sanders[6] and Fujita[10b] have shown that synthetic hosts can affect DA *exo*/*endo*- and regio-selectivity, respectively, neither example exhibit turnover. We were therefore keen to demonstrate specificity bias under sub-stoichiometric conditions. Where diasteroselectivity can be readily determined (i.e., all reactions of dienes **3**, **4** and **8**), in all cases the uncatalyzed and catalyzed reactions are 100% *endo* selective.[22]

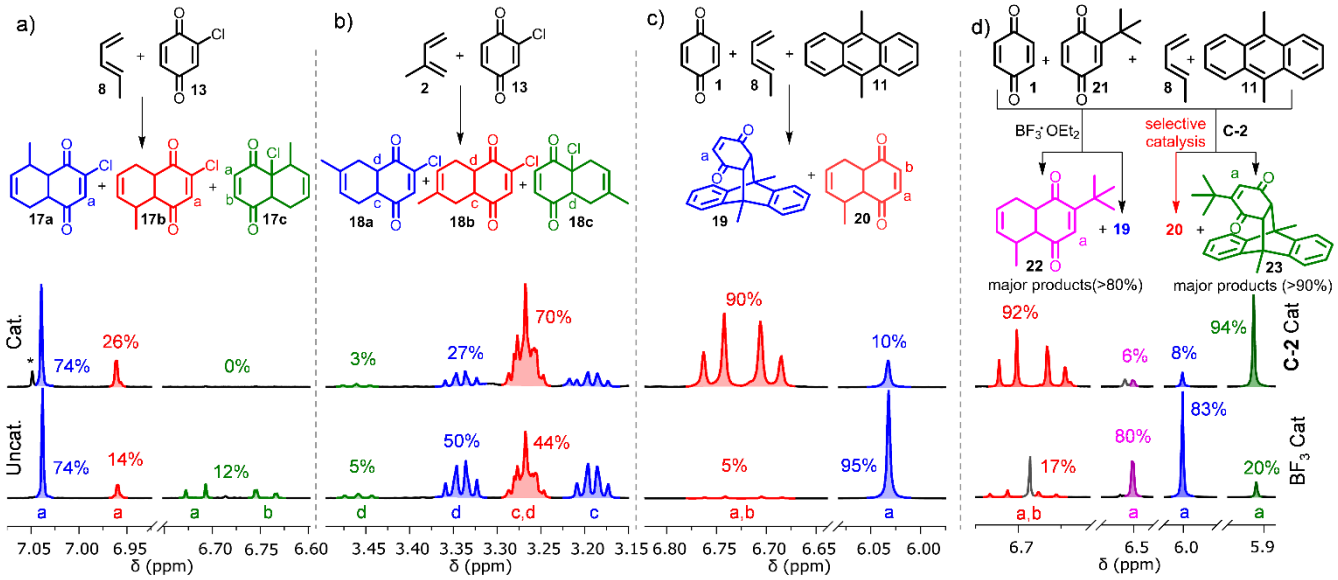

Figure 6. Capsule catalyzed modulation of selectivity. Product distributions for catalyzed (20 mol%) and uncatalyzed reactions determined by ^{1}H NMR integration. (a-b) Regiochemical switching of remote substituents (Cl, Me). (c) **C-2** completely alters the chemoselectivity of bulky diene **11** and the small but intrinsically less reactive **8**. (d) While small-molecule catalysis ($BF_3{\cdot}OEt_2$) promotes conventional selectivity of most reactive substrates (**1** and **11**), **C-2** enhances a different reaction. Note: **21** is not a guest for **C-2**. Excess equimolar dienes used for **C-2** catalyzed / uncatalyzed chemoselective reactions to drive to completion with respect to quinone starting materials. *Solvent spinning sideband.

It is perhaps not unsurprising that **C-2** does not perturb the intrinsic *endo* preference, as the *exo* TS is less compact and therefore likely to be less well accommodated by the cavity of **C-2**. However, while **C-2** does not modulate diasteroselectivity with these substrates, we do observe that it can alter regio-, site- and chemo-selectivity under true catalytic conditions (20 mol%). With the reaction of **13** and **8**, the uncatalyzed reaction produces isomers **17a-c** (Figure 6a), however, **17c** is completely suppressed in the presence of **C-2**, possibly due to the steric confinement preventing C-C bond formation between adjacent methyl and chloro-substituents. The loss of **17c** is also accompanied by an increase in the proportion of the other less favored species, **17b**. While the precise reasons for this switch are probably complex and multi-tiered, the trend appears to be that **C-2** favors an increased proportion of products with more "transoid" arrangement of substituents. This is even more noticeable with the reaction of **2** and the same quinone **13**, which produces a larger regioselective switch under catalytic conditions (Figure 6b). Here, the intrinsically less favored "para" isomer **18b** is favored by 3:1 over "meta" **18a** in the presence of **C-2**. This is a significant change considering the remoteness of the substituents that define this regiochemistry. Finally, we also envisaged that the microenvironment could be used to catalytically influence chemoselectivity. When reactive but bulky diene **11** is competed with smaller but less reactive **8** for cycloaddition with **1** under catalyst-free conditions, almost complete selectivity (>95%) for anthracene adduct **19** (Figure 6c) was observed. However, 20 mol% **C-2** gives almost complete reversal of this selectivity, producing **20** in 90% yield. This is not solely a result of **C-2** protecting the dienophile from reaction with the most reactive diene,[23] but additionally accelerating the less-favored bulk-phase process thus showing that the capsule can reverse the intrinsic reactivity of different dienes. We can also add another level of complexity to this reaction by including a second dienophile, *t*-butylbenzoquinone **21** (Figure 6d), which is not a guest for **C-2**. When these substrates are reacted in a stoichiometric ratio under non-catalytic conditions, this bulk-phase process is very slow. However, in the presence of a conventional Lewis-acid catalyst, $BF_3{\cdot}OEt_2$, all four possible products are observed, with a significant excess of **19** and **22**. This bias is a consequence of preferred cycloaddition between most reactive diene and dienophile pair (**11** and **1**), which then leaves a higher concentration of least reactive substrates (**21** and **8**). When $BF_3{\cdot}OEt_2$ is changed for 20 mol% **C-2**, the intrinsically less-favored **20** and **23** are produced with greater selectivity (>90%), showing the capsule is able to selectively accelerate one of the least favored out of the four possible reactions. The amplification of a single reaction from a collection of substrates that otherwise show similar reactivity is a frequent hallmark of biological processes, from biosynthesis though to signaling mechanisms, and almost impossible to achieve using conventional catalytic approaches. The credentials of this current system thus pave the way to various opportunities, from complex synthetic cascades though to molecular sensing.

Conclusions

While artificial receptors that co-bind diene and dienophile substrates frequently show increased DA reactivity, this "bio-inspired" approach is invariably hindered by severe product inhibition. In contrast, we have shown that a simple quinone-binding Pd_2L_4 capsule system can promote enclosed catalysis with efficient turnover by negating the need to formally co-bind the diene component. Instead, increased reactivity is provided by a convergent array of weak H-bond donor and acceptor groups, which stabilize the cycloaddition pathway. The influence the microenvironment has on catalysis is profound; together, the collection of interactions lowers the free energy of activation to an extent only previously observed in catalytic antibodies, and more recently in naturally occurring intramolecular Diels–Alderases.[19] We have also shown that the enclosed environment is able to influence regio- and chemo-selectivity in

a way that simple small molecules systems could not. We envisage that the transition from entropic to enthalpic capsule catalytic models will be widely applicable to a range of different reaction types.

Experimental Methods

General. All reagents and solvents were purchased from Alfa Aesar, VWR or Sigma Aldrich and used without further purification, except **1**, which was recrystallized form hot CH_2Cl_2/pet ether 60-80 (1:5) and **14**, which was recrystallized form hot CH_2Cl_2/pet ether 60-80 (1:3). Cage **C-1** was prepared using the previously reported method.[15b]

All ^1H, ^{13}C and ^{19}F NMR spectra were recorded on either a 500 MHz Bruker AV III equipped with a DCH cryo-probe (Ava500), a 500 MHz Bruker AV IIIHD equipped with a Prodigy cryo-probe (Pro500), a 600 MHz Bruker AV IIIHD equipped with a TCI cryo-probe (Ava600) or a 400 MHz Bruker AV III equipped with BBFO+ probe (Ava400) at a constant temperature of 300 K. Chemical shifts are reported in parts per million. Coupling constants (J) are reported uncorrected in hertz (Hz). Apparent multiplicities are reported using the following standard abbreviations: m = multiplet, q = quartet, t = triplet, d = doublet, s = singlet, bs = broad singlet. All analysis was performed with MestReNova, version 11. For full assignment(s), see the Supporting Information. These were made using a combination of COSY, NOESY, HSQC and HMBC NMR spectra. MS was performed on a Synapt G2 (Waters, Manchester, UK) mass spectrometer, using a direct infusion electrospray ionization source (ESI), controlled using Masslynx v4.1 software.

Synthesis of C-2. The cage **C-2**·4OTf was prepared according to a literature method.[24] To a solution of **C-2**·$(OTf)_4$ (147 mg, 75.9 μmol, 1 equiv) in CH_2Cl_2 (40 mL) was added NaBArF (269 mg, 307 μmol, 4 equiv), which was then sonicated for 5 min. The reaction mixture was filtered and the undissolved material washed with further CH_2Cl_2 (150 mL). The solvent was removed under reduced pressure to obtain **C-2** (cage·$(BArF)_4$) as an off white solid (333 mg, 69.4 μmol, 91% yield). ^1H NMR (500 MHz, CD_2Cl_2): δ 8.88 (s, 8H), 8.57 (d, J = 5.5 Hz, 8H), 8.08 (dt, J = 8.1, 1.5 Hz, 8H), 7.77–7.72 (m, 4H), 7.72 – 7.67 (m, 32H, H_{BArF}), 7.58–7.52 (m, 12H), 7.52 ppm (s, 16H, H_{BArF}). For a full assignment, see the SI. ^{13}C NMR (126 MHz, CD_2Cl_2): δ 162.29 (q, $J_{C–F}$ = 50.0 Hz, BArF), 152.74, 149.12, 145.52, 142.16, 138.34, 135.34 (m, BArF), 130.00–128.27 (m, BArF), 129.58, 129.13, 125.99, 125.10 (q, $J_{C–F}$ = 272.5 Hz, BArF), 118.27–117.86 (m, BArF), 96.70, 81.52 ppm. ^{19}F NMR (471 MHz, CD_2Cl_2): δ –62.75 ppm. ^1H DOSY NMR (500 MHz, CD_2Cl_2): 4.32×10^{-10} m^2/s, hydrodynamic radius = 12.1 Å. ESI TOF HRMS m/z: Found 3922.3789 $[M–BArF]^+$, calculated for $[C_{172}H_{80}B_3F_{72}N_{12}Pd_2]^+$ 3927.3928. Found 1532.1631 $[M–2BArF^-]^{2+}$, calculated for $[C_{140}H_{68}B_2F_{48}N_{12}Pd_2]^{2+}$ 1532.1548. Found 733.7532 $[M–3BArF]^{3+}$, calculated for $[C_{108}H_{56}BF_{24}N_{12}Pd_2]^{3+}$ 733.7559. Found 334.2973 $[M–4BArF]^{4+}$, calculated for $[C_{76}H_{44}N_{12}Pd_2]^{4+}$ 334.2977.

Experimental determination of kinetic constants

All kinetic constants were determined the following general procedure. To an NMR tube was introduced either a solution containing the cage (**C-1** or **C-2**) compound (450 μL of a stock 0.56 mM solution in CD_2Cl_2) or just CD_2Cl_2 (450 μL) for the uncatalyzed reactions, quinone (20 μL of a 62.5 mM stock solution in CD_2Cl_2), and the internal standard tetrakis(trimethylsilyl)silane (10 μL of a 15.2 mM stock solution in CD_2Cl_2). For the reactions with the competitive inhibitor, solid anthraquinone **S13** was added to the NMR tube (5.2 mg, 25 μmol). The Diels–Alder reaction was then started by the addition of the corresponding diene (20 μL of a stock solution in CD_2Cl_2, 5–100 equivalents depending on diene reactivity). ^1H NMR spectra were recorded at regular intervals until sufficient data was collected to determine the kinetic parameters. In all cases the NMR reactions were kept at 298 K. Kinetic NMR data was processed using the MestreNova 11 software and the concentration of all chemical species were determined for each reaction time. All reactions were performed at least twice and a representative example is reported in the supporting information.

Experimental kinetic constants for the catalyzed reaction (k_{cat}) were obtained by fitting to the simulated kinetic model using the Levenberg-Marquardt Nonlinear Least-Squares Algorithm[25] implemented in the R software[26] and the RStudio[27] software interface. Fittings were carried out simultaneously to total product and quinone concentration (due to fast exchange of these guests on the NMR timescale) in order to both minimize the mathematical fitting errors and also ensure that the data fit to the kinetic model. For more information see the supporting Information. The association constants of the quinones were determined by ^1H NMR titrations while the association constants of the Diels–Alder adducts ($K_{P\ Ass}$) were determined either by similar titrations or by estimation from fitting the kinetic data (see Supporting Information). Initial rates (V_{max}) of the catalyzed and uncatalyzed reactions were calculated from the slope obtained by linear fitting to the initial data points of the reaction ($[quinone]_{total}$ vs. time).The associated Gibbs energy barrier ($\Delta G^{\ddagger}$) for each the kinetic constant (k) and additional parameters determined from the kinetic constants were calculated as described in the supporting information.

ASSOCIATED CONTENT

Supporting Information

The Supporting Information is available free of charge on the ACS Publications website. This includes synthetic details and characterization, binding constant and kinetic experiments

AUTHOR INFORMATION

Corresponding Author

Paul.Lusby@ed.ac.uk

Paul Lusby ORCID ID: https://orcid.org/0000-0001-8418-5687

Vicente Martí-Centelles ORCID ID: https://orcid.org/0000-0002-9142-9392

Andrew L. Lawrence ORCID ID: http://orcid.org/0000-0002-9573-5637

Notes

The authors declare no competing financial interests.

ACKNOWLEDGMENT

This work was supported by the Leverhulme Trust (RPG-2015-232).

ABBREVIATIONS

DA, Diels-Alder; LUMO, lowest unoccupied molecular orbital; NMR, Nuclear Magnetic Resonance; TON, turnover number, TS, transition state.

REFERENCES

(1) (a) Michael, J. W.; Ulmann, P. A.; Mirkin, C A. *Angew. Chem. Int. Ed.* **2011**, *50*, 114. (b) Slagt, V. F.; Reek, J. N. H.; Kamer, P. C. J.; van Leeuwen, P. W. N. M. *Angew. Chem. Int. Ed.* **2001**, *40*, 4271. (c) Lee, S. J.; Cho, S.-H.; Mulfort, K. L.; Tiede, D.M.; Hupp, J. T.; Nguyen, S. T. *J. Am. Chem. Soc.* **2008**, *130*, 16828. (d) Kaphan, D. M.; Levin, M. D.; Bergman, R. G.; Raymond, K. N.; Toste, F. D. *Science* **2015**, *350*, 1235. (e) Zhang, Q.; Tiefenbacher, K. *Nat. Chem.* **2015**, *7*, 197. (f) Wang, Q.-Q.; Gonell, S.; Leenders, S. H. A. M.; Dürr, M.; Ivanović-Burmazović, I.; Reek, J. N. H. *Nat. Chem.* **2016**, *8*, 225. (g) Omagari, T.; Suzuki, A.; Akita, M.; Yoshizawa, M. *J. Am. Chem. Soc.* **2016**, *138*, 499.

(2) (a) Yoshizawa, M.; Klosterman, J. K.; Fujita, M. *Angew. Chem. Int. Ed.* **2009**, *48*, 3418. (b) Chakrabarty, R.; Mukherjee, P. S.; Stang, P. J. *Chem. Rev.* **2011**, *111*, 6810. (c) Ward, M. D.; Raithby, P. R. Chem. Soc. Rev. **2013**, *42*, 1619. (d) Cook, T. R.; Stang, P. J. *Chem. Rev.* **2015**, *115*, 7001; (e) Brown, C. J.; Toste, F. D.; Bergman, R. G.; Raymond, K. N., *Chem. Rev.,* **2015**, *115*, 3012. (f) Zarra, S.; Wood, D. M.; Roberts, D. A.; Nitschke, J. R. *Chem. Soc. Rev.* **2015**, *44*, 419. (g) Otte, M. *ACS Catalysis* **2016**, *6*, 6491. (h) Bloch, W. M.; Clever, G. H. *Chem. Commun.***, 2017**, *53*, 8506.

(3) Rideout, D. C.; Breslow, R. *J. Am. Chem. Soc.* **1980**, *102*, 7817.

(4) Kelly, T. R.; Zhao, C.; Bridger, G. J. *J. Am. Chem. Soc.* **1989**, *111*, 3744.

(5) Tjivikua, T.; Ballester, P.; Rebek Jr., J. *J. Am. Chem. Soc.* **1990**, *112*, 1249.

(6) Waiter, C. J.; Anderson, H. L.; Sanders, J. K. M. *J. Chem. Soc., Chem. Commun.***1993**, 458.

(7) (a) Kang, J.; Rebek Jr., J. *Nature* **1997**, *385*, 50.; (b) Chen, J.; Rebek Jr, J. *Org. Lett.* **2002**, *4*, 327.

(8) (a) Yoshizawa, M.; Takeyama, Y.; Okano, T.; Fujita, M. *J. Am. Chem. Soc.* **2003**, *125*, 3243; (b) Nishioka, Y.; Yamaguchi, T.; Yoshizawa, M.; Fujita, M. *J. Am. Chem. Soc.* **2007**, *129*, 7000. (c) Murase, T.; Horiuchi, S.; Fujita, M. *J. Am. Chem. Soc.* **2010**, *132*, 2866.

(9) Parthasarathy, A.; Kaanumalle, L. S.; Ramamurthy, V. *Org. Lett.* **2007**, *9*, 5059.

(10) (a) Kang, J.; Santamaria, J.; Hilmersson, G.; Rebek Jr.; *J. Am. Chem. Soc.* **1998**, *120*, 7389. (b) Yoshizawa, M.; Tamura, M.; Fujita, M. *Science* **2006**, *312*, 251.

(11) (a) Pluth, M. D.; Bergman, R. G.; Raymond, K. N. *Angew. Chem. Int. Ed.* **2007**, *46*, 8587. (b) Bolliger, J. L.; Belenguer, A. M.; Nitschke, J. R. *Angew. Chem. Int. Ed.* **2013**, *52*, 7958.

(12) (a) Salles, A. G.; Zarra, S.; Turner, R. M.; Nitschke, J. R. *J. Am. Chem. Soc.* **2013**, *135*, 19143. (b) Cullen, W.; Misuraca, M. C.; Hunter, C. A.; Williams, N. H.; M. D. Ward, *Nat. Chem.* **2016**, *8*, 231.

(13) (a) Fiedler, D.; Bergman, R. G.; Raymond, K. N. *Angew. Chem. Int. Ed*. **2004**, *43*, 6748.

(14) (a) Pluth, M. D.; Bergman, R. G.; Raymond, K. N. *Science* **2007**, *316*, 85. (b) Hastings, C. J.; Pluth, M. D.; Bergman, R. G.; Raymond, K. N. *J. Am. Chem. Soc.* **2010**, *132*, 6938. (c) Murase, T.; Nishijima, Y.; Fujita, M. *J. Am. Chem. Soc.* **2011**,*134*, 162.

(15) (a) Liao, P.; Langloss, B. W.; Johnson, A. M.; Knudsen, E. R.; Tham, F. S.; Julian, R. R.; Hooley, R. J. *Chem. Commun.* **2010**, *46*, 4932. (b) August, D. P.; Nichol, G. S.; Lusby, P. J. *Angew. Chem. Int. Ed.* **2016**, *55*, 15022. (c) Lewis, J. E. M.; Gavey, E. L.; Cameron, S. A.; Crowley, J. D. *Chem. Sci.* **2012***, 3*, 778.

(16) Wittkopp, A.; Schreiner, P. R. *Chem. Eur. J.* **2003**, *9*, 407.

(17) For a H-bond cavitand that activates partially encapsulated maleimide dienophiles, see Hooley, R. J.; Rebek Jr., J. *Org. Biomol. Chem.* **2007**, *5*, 3631.

(18) (a) Pauling, L. *Nature* **1948**, *161*, 707. For an example of recent supramolecular TS stabilization of DA reactions using anion-π interactions, see (b) Liu, L.; Cotelle, Y.; Bornhof, A.-B.; Besnard, C.; Sakai, N.; Matile, S. *Angew. Chem. Int. Ed.* **2017**, *56*, 13066.

(19) It is likely that similar product conformational changes allow naturally-occurring Diels–Alderase enzymes to turnover. For a recent example, see Byrne, M. J.; Lees, N. R.; Han, L.-C.; van der Kamp,M. W.; Mulholland, A. J.; Stach, J. E. M.; Willis, C. L.; Race, P. R. *J. Am. Chem. Soc.* **2016**, *138*, 6095.

(20) Palma, A.; Artelsmair, M.; Wu, G.; Lu, X.; Barrow, S. J.; Uddin, N.; Rosta, E.; Masson, E.; Scherman, O. A. *Angew. Chem. Int. Ed*. **2017**, *56*, 15688.

(21) Kim, S. P.; Leach, A. G.; Houk, K. N. *J. Org. Chem.* **2002**, *67*, 4250.

(22) In the case of the catalyzed reaction of **1** and **8**, we observe the formation of a single diastereomer (see SI). This strongly suggests that **C-2** is catalyzing a concerted [4+2] cycloaddition and not a stepwise reaction.

(23) Smulders, M. M. J.; Nitschke, J. R. *Chem. Sci.* **2012**, *3*, 785.

(24) M. Lewis, J. E.; Crowley, J. D. *Supramol. Chem.* **2014**, *26*, 173–181.

(25) Elzhov, T. V.; Mullen, K. M.; Spiess, A.-N.; Bolker, B. *minpack.lm: R Interface to the Levenberg-Marquardt Nonlinear Least-Squares Algorithm Found in MINPACK, Plus Support for Bounds*. R package version 1.2-0, 2015. https://CRAN.R-project.org/package=minpack.lm (accessed January 23, 2018).

(26) R Core Team. *R: A language and environment for statistical computing*. R Foundation for Statistical Computing: Vienna, Austria, 2015. https://www.R-project.org/ (accessed January 23, 2018).

(27) Studio Team. *RStudio: Integrated Development for R, version 0.99.892*. RStudio, Inc.: Boston, MA, 2015. http://www.rstudio.com/ (accessed January 23, 2018).

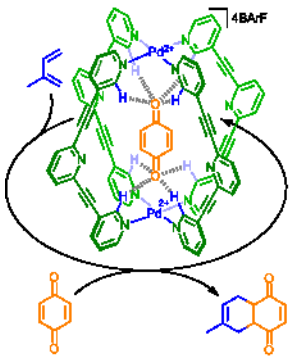

+ Low product Inhibition (TON ≈ 1000)

+ High activity (k_{cat}/k_{uncat} > 1000)

+ Interesting and selective "enclosed" reactivity